Reprinted from October 1976, Vol. 98, Journal of Engineering Materials and Technology

# Fully Plastic Solutions and Large Scale Yielding Estimates for Plane Stress Crack Problems[1]

**C. F. SHIH**

Corporate Research and Development Center, General Electric Co., Schenectady, N. Y.

**J. W. HUTCHINSON**

Division of Engineering and Applied Physics, Harvard University, Cambridge, Mass.

*Fully plastic plane stress solutions are given for a center-cracked strip in tension and an edge-cracked strip in pure bending. In the fully plastic formulation the material is characterized by a pure power hardening stress-strain relation which reduces at one limit to linear elasticity and at the other to rigid/perfect plasticity. Simple formulas are given for estimating the J-integral, the load-point displacement and the crack opening displacement in terms of the applied load for strain hardening materials characterized by the Ramberg-Osgood stress-strain relation in tension. The formulas make use of the linear elastic solution and the fully plastic solution to interpolate over the entire range of small and large scale yielding. The accuracy of the formulas is assessed using finite element calculations for some specific configurations.*

## Introduction

In reference [1][2] a relatively simple procedure has been proposed for estimating solutions to large scale yielding crack problems where the load is monotonically increased and the crack is stationary. The method accounts for strain hardening and makes use of two special solutions, the elastic solution and the fully plastic solution, to interpolate over the entire range of yielding. In [1] the simple estimates were compared with full numerical calculations for antiplane shear problems. For relations between quantities of primary interest in fracture mechanics (i.e., the applied load, the crack opening displacement, $J$, and the load point displacement), the simple formulas were found to be quite accurate.

In this paper the study is extended to plane stress problems. Numerical results are first presented for the fully plastic solutions to two crack configurations: the center-cracked strip and the single edge-cracked strip in bending. Using these solutions, large scale yielding estimates are made for each of the configurations and, to assess their accuracy, they are compared with full numerical calculations. The tensile behavior of the material is taken to be characterized by the Ramberg-Osgood relation and, in the full numerical calculations, $J_2$ deformation theory is used to generalize this relation to multiaxial stress states.

## Center-Cracked Strip

**Fully Plastic Solution.** What is referred to here as the fully plastic problem is the small strain problem for a nonlinear material which behaves in simple tension according to the pure power hardening law

$$\epsilon/\epsilon_0 = \alpha(\sigma/\sigma_0)^n \tag{1}$$

where $\sigma_0$ and $\epsilon_0$ are reference values, $\alpha$ is a constant and $n$ is the hardening exponent. At one limit, $n = 1$, (1) represents linear behavior and at the other, $n \to \infty$, it gives rigid/perfectly plastic behavior. The uniaxial behavior is generalized to multiaxial states using $J_2$ deformation theory:

$$\epsilon_{ij}/\epsilon_0 = \frac{3}{2}\alpha(\sigma_e/\sigma_0)^{n-1}s_{ij}/\sigma_0 \quad \text{with} \quad \sigma_e = \sqrt{\left(\frac{3}{2}\, s_{ij}s_{ij}\right)} \tag{2}$$

where $s_{ij}$ is the stress deviator. A general discussion of the features of crack problems involving the above constitutive behavior is given in [2]. Here we consider a strip of width $2b$ with a traction-free center crack of length $2a$ centered at the coordinate origin with $x_2$ taken to be normal to the crack. The strip is

[1]This work was supported in part by the Air Force Office of Scientific Research under Grant AFOSR-73-2476, in part by the Advanced Research Projects Agency under Contract F44620-75-C-0088, and by the Division of Engineering and Applied Physics, Harvard University.

[2]Numbers in brackets designate References at end of paper.

Contributed by the Materials Division for publication in the JOURNAL OF ENGINEERING MATERIALS AND TECHNOLOGY. Manuscript received by the Materials Division, September 2, 1975; revised manuscript received November 24, 1975. Paper No. 76-Mat-P.

subject to uniform stress $\sigma_{22} \to \sigma^\infty$ for $|x_2| \to \infty$.

As discussed in [2], the solution to this boundary value problem has the property that all stress quantities are linearly proportional to $\sigma^\infty$ and all strain and displacement quantities are proportional to $(\sigma^\infty)^n$. One consequence of this property is that, if $\sigma^\infty$ is monotonically applied, the solution is also an exact solution for $J_2$ flow theory. Another consequence is the simple functional relation between the quantities of interest. It is this feature which makes these solutions attractive for use in estimating large scale yielding behavior. For the quantities of primary interest the following normalizations have been found to be useful [1, 2]

$$J = \alpha\sigma_0\epsilon_0 a(1 - a/b)g_1(a/b, n)(P/P_0)^{n+1} \tag{3}$$

$$\delta = \alpha\epsilon_0 a g_2(a/b, n)(P/P_0)^n \tag{4}$$

$$\Delta_e = \alpha\epsilon_0 a g_3(a/b, n)(P/P_0)^n \tag{5}$$

where the $g$'s are functions of $a/b$ and $n$ alone. Here $P$ is the total load per unit thickness and $P_0$ is a reference load per unit thickness:

$$P = 2b\sigma^\infty,\ P_0 = 2(b - a)\sigma_0 \tag{6}$$

For the rigid-perfectly plastic limit ($n \to \infty$), $P_0$ is the limit load. Generally, $P/P_0 = [\sigma^\infty b/(b - a)]/\sigma_0$ is the net section stress divided by the reference stress $\sigma_0$ and this ratio enters naturally in arriving at the normalizations (3)–(5) as discussed in [2]. In (3), $J$ is the $J$-integral [3] whose significance in the present context is that it is a measure of the strength of the dominant singularity at the crack tip. In (4), $\delta = u_2(0, 0^+) - u_2(0, 0^-)$ is the crack opening displacement at the center of the crack. The residual load point displacement is denoted by $\Delta_e$ and is defined as follows. For a finite length strip, $-h \le x_2 \le h$, with $\sigma_{22} = \sigma^\infty$ prescribed on its ends, define $\Delta(h)$ as the load point displacement, i.e.,

$$\Delta(h) = \frac{1}{2b}\int_{-b}^{b} [u_2(x_1, h) - u_2(x_1, -h)]dx_1 \tag{7}$$

The load point displacement for an uncracked strip of length $2h$ is $\Delta_{\text{no crack}} = 2h\epsilon^\infty$, where $\epsilon^\infty$ is $\epsilon_{22}$ component of strain due to $\sigma^\infty$. The residual load point displacement is defined as

$$\Delta_e = \lim_{h\to\infty} [\Delta(h) - \Delta_{\text{no crack}}] \tag{8}$$

Thus, for a strip of length $2h$,

$$\Delta(h) \cong \Delta_{\text{no crack}} + \Delta_e \tag{9}$$

where the error in (9) is small if $h$ is sufficiently large compared to $b$ or, in certain instances, $b - a$.

Values of $g_1$, $g_2$, and $g_3$ have been calculated for a wide range of values of $a/b$ and $n$ (see Table 1 and Fig. 1) using a finite element method which employs a singular crack-tip element. The plane stress calculations carried out here are similar in principle to the anti-plane shear calculations discussed in some detail in [1]. Over the range $1/8 \le a/b \le 3/4$ and $1 \le n \le 20$, the finite element results for the analogous fully plastic and anti-plane shear problem were in almost all cases within 2 or 3 percent of subsequently obtained exact results [7] and were never more than 6 percent in error. The accuracy of the present results should be comparable. For the linear case, $n = 1$, the results agree to within 2 percent with the widely used results of [5] and [6]. The result of [6] which is claimed to be accurate to within 0.3 percent can be expressed in the present notation as

$$J = \alpha\sigma_0\epsilon_0 a(1 - a/b)g_1(a/b, 1)(P/P_0)^2 \tag{10}$$

where

$$g_1(a/b, 1) = \pi[1 - 0.5a/b - 0.370(a/b)^2 - 0.044(a/b)^3]^2 \tag{11}$$

A finite length strip with $h/b = 3$ was used in all calculations with uniform $\sigma_{22}$ prescribed on the ends. In the linear case ($n = 1$) the choice of $h/b = 3$, by itself, is thought to contribute an error of less than 1/2 percent in the quantities $J$, $\delta$, and $\Delta_e$ compared with the limit results for $h/b = \infty$ [6]. In the nonlinear cases ($n > 1$) the error due to this length truncation should be even less due to the high degree of localization of the deformation in the region ahead of the crack. For $n \to \infty$, a diffuse "neck" forms ahead of the crack (see ahead to insert of Fig. 3). The solid line portions of the curves in Fig. 1 are plots of the numerical results from Table 1 and the dashed line portions are obtained by extrapolation in the manner discussed below.

While the normalizations in (3)–(5) are convenient for the purposes of the next section, they do not provide much indication of the relations for $n > 10$, nor do they permit extrapolation to the limiting cases $a/b = 0$ and $a/b = 1$. The exact solution to the analogous anti-plane shear problem solved by Amazigo [7] suggests an alternative to (3) for normalizing $J$. A slab of width $2b$ with a center crack of length $2a$ is subject to an anti-plane shearing stress $\tau^\infty$ at infinity. The material of the slab is governed by $J_2$ deformation theory with the pure shear relation $\gamma/\gamma_0 = \alpha(\tau/\tau_0)^n$. The analog to (3) for the anti-plane problem is

**Table 1**

| | | $1/n = 1$ | 0.667 | 0.5 | 0.333 | 0.2 | 0.143 | 0.1 |
|---|---|---|---|---|---|---|---|---|
| | | $n = 1$ | 1.5 | 2 | 3 | 5 | 7 | 10 |
| $a/b = 0$ | G | 1.0 | 1.03 | 1.02 | 1.01 | 1.005 | 1.00 | 1.00 |
| $a/b = 1/8$ | $g_1$ | 2.800 | 3.231 | 3.543 | 4.00 | 4.518 | 4.761 | 4.861 |
| | $g_2$ | 3.532 | 3.867 | 4.107 | 4.464 | 4.827 | 4.945 | 4.894 |
| | $g_3$ | 0.347 | 0.491 | 0.640 | 0.949 | 1.537 | 2.048 | 2.630 |
| | G | 1.0 | 1.022 | 1.010 | 1.004 | 1.031 | 1.069 | 1.114 |
| $a/b = 1/4$ | $g_1$ | 2.544 | 2.820 | 2.972 | 3.140 | 3.195 | 3.106 | 2.896 |
| | $g_2$ | 3.116 | 3.235 | 3.286 | 3.304 | 3.151 | 2.926 | 2.595 |
| | $g_3$ | 0.611 | 0.820 | 1.010 | 1.352 | 1.830 | 2.083 | 2.191 |
| | G | 1.0 | 1.014 | 1.004 | 1.008 | 1.037 | 1.059 | 1.072 |
| $a/b = 1/2$ | $g_1$ | 2.211 | 2.242 | 2.195 | 2.056 | 1.811 | 1.643 | 1.465 |
| | $g_2$ | 2.382 | 2.182 | 2.003 | 1.703 | 1.307 | 1.084 | 0.892 |
| | $g_3$ | 0.924 | 1.085 | 1.180 | 1.254 | 1.183 | 1.051 | 0.888 |
| | G | 1.0 | 0.994 | 0.975 | 0.952 | 0.939 | 0.944 | 0.957 |
| $a/b = 3/4$ | $g_1$ | 2.073 | 1.893 | 1.708 | 1.458 | 1.208 | 1.082 | 0.956 |
| | $g_2$ | 1.611 | 1.215 | 0.970 | 0.685 | 0.452 | 0.361 | 0.292 |
| | $g_3$ | 0.933 | 0.886 | 0.802 | 0.642 | 0.450 | 0.361 | 0.292 |
| | G | 1.0 | 0.977 | 0.931 | 0.880 | 0.860 | 0.875 | 0.895 |
| $a/b = 1$ | G | 1.0 | 0.966 | 0.880 | 0.805 | 0.80 | 0.83 | 0.86 |

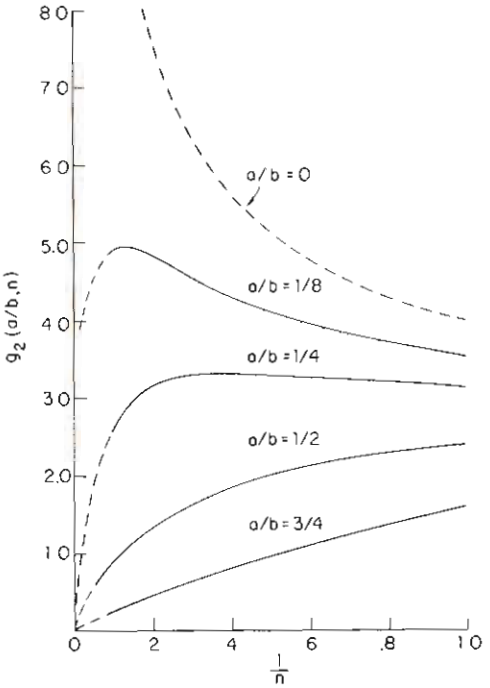


**Fig. 1 Plots of $g_1$ and $g_2$ as defined in equations (3) and (4). Dashed line segments are extrapolated as discussed later in text.**

$$J = \alpha\tau_0\gamma_0 a(1 - a/b)q(a/b, n)(P/P_0)^n \tag{12}$$

where now $P = 2b\tau^\infty$ and $P_0 = 2(b - a)\tau_0$ and values of $q$ are given in [7]. The exact result for $n = 1$ is

$$q(a/b, 1) = (b/a - 1)\tan(\pi a/2b) \tag{13}$$

The asymptotic results of [4, 7] for the large $n$ behavior of $q$ indicate a nonuniform limit depending on whether $a/b$ is zero or not. For large $n$ Amazigo's results indicate

$$q(a/b, n) \sim c\sqrt{n}/[1 + \zeta(n - 1)a/b] \tag{14}$$

where $\zeta = \sqrt{e} = 1.6487$ and $c = (\pi/2)^{3/2} = 1.9687$. Consider the function $Q(a/b, n)$ defined in terms of $q$ by the equation

$$Q(a/b, n) = q(a/b, n)\left[\frac{1 + \zeta(n - 1)a/b}{c\sqrt{n}(1 - 1/n) + q(a/b, 1)/\sqrt{n}}\right] \tag{15}$$

Equation (15) is composed such that $Q(a/b, 1) = 1$ for all $a/b$, and, from (14), $Q(a/b, n) \to 1$ as $n \to \infty$ for all $a/b$. Curves of $Q$ against $1/n$ for fixed $a/b$ have been calculated from the exact results of [7] and are shown in Fig. 2(*a*). The function $Q$ collapses the anti-plane shear results to within a relatively small variation from unity for all values of $a/b$ and $n$. Given $Q(a/b, n)$ one can work backwards and obtain $J$ from (12), (13), and (15).

We now attempt to find a scaling function $G(a/b, n)$ for the plane stress results under the unproven assumption that $J$ depends functionally on large $n$ in the same nonuniform way as in (14). Based on (15) we try

$$G(a/b, n) = g_1(a/b, n)\left[\frac{1 + \zeta(n - 1)a/b}{c\sqrt{n}(1 - 1/n) + g_1(a/b, 1)/n}\right] \tag{16}$$

Now, $\zeta$ and $c$ are free constants to be chosen such that the numerical results for $G$, calculated from (16) using the values of $g_1$ from Table 1, extrapolate to unity for all $a/b$ as $n \to \infty$. It was found that (16) could indeed scale the plane stress numerical results of the table. The best choice of the constants was found to be $\zeta = 1.40$ and $c = 3.85$, and curves of $G$ are shown in

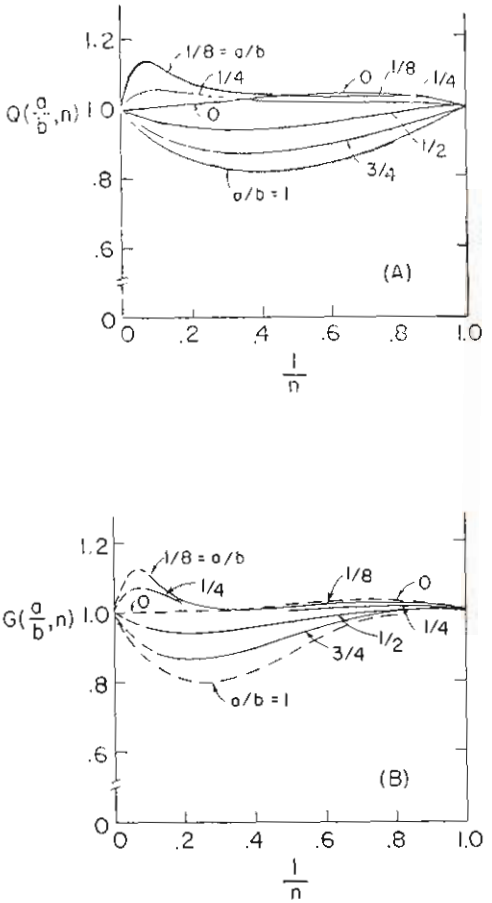


**Fig. 2 (*a*) Amazigo's [7] exact results for anti-plane shear normalized using $Q(a/b, n)$ as defined in equation (15). (*b*) Plane stress values normalized using $G(a/b, n)$ defined in equation (16).**

Fig. 2(*b*). The close similarity in almost every detail, especially for high $n$-values, with the anti-plane shear results of Fig. 2(*a*) suggests that (16) may embody the correct functional behavior of $J$ for large $n$ for plane stress as well as anti-plane shear. Dashed line segments of curves in Fig. 2(*b*) are extrapolated. The curve for $a/b = 1$ was obtained with no difficulty by cross-plotting for fixed $n$ and extrapolating the values for $a/b = 1/4$, $1/2$ and $3/4$ to 1. For $n > 3$ it is not possible to extrapolate to $a/b = 0$ by this same process (as is also clear from the exact values for anti-plane shear in Fig. 2(*a*)). In this case we have drawn on the striking similarity between the two families of curves and have, with no further justification, drawn in the segment of the curve for $a/b = 0$ above $n = 3$ in the same way as it appears in Fig. 2(*a*) for anti-plane shear. The values of $G$ thus obtained were used to calculate, from (16), values of $g_1$ for $a/b = 0$ and $a/b = 1$ shown in Fig. 1.

Since $G(0, n)$ as plotted in Fig. 2(*b*) differs from unity by no more than 4 percent over the entire range of $n$, we can, as an approximation, take it to be unity and thus, from (3) and (16), obtain the following relatively simple formula for $J$ for the finite crack in an infinite sheet

$$J = \alpha\sigma_0\epsilon_0 a[3.85\sqrt{n}(1 - 1/n) + \pi/n](\sigma^\infty/\sigma_0)^{n+1} \tag{17}$$

Scalings similar to those in (15) and (16) can also be constructed for the crack opening displacement $\delta$. In doing so it is useful to note the following limiting relation for a rigid/perfectly plastic strip [8], valid for all $a/b$,

$$J = \sigma_0\delta = \sigma_0\Delta_c \tag{18}$$

An approximation to $\delta$ for $a/b = 0$, obtained in the same manner as (17), is

$$\delta = \alpha\epsilon_0 a[3.85\sqrt{n}(1 - 1/n) + 4/n](\sigma^\infty/\sigma_0)^n \tag{19}$$

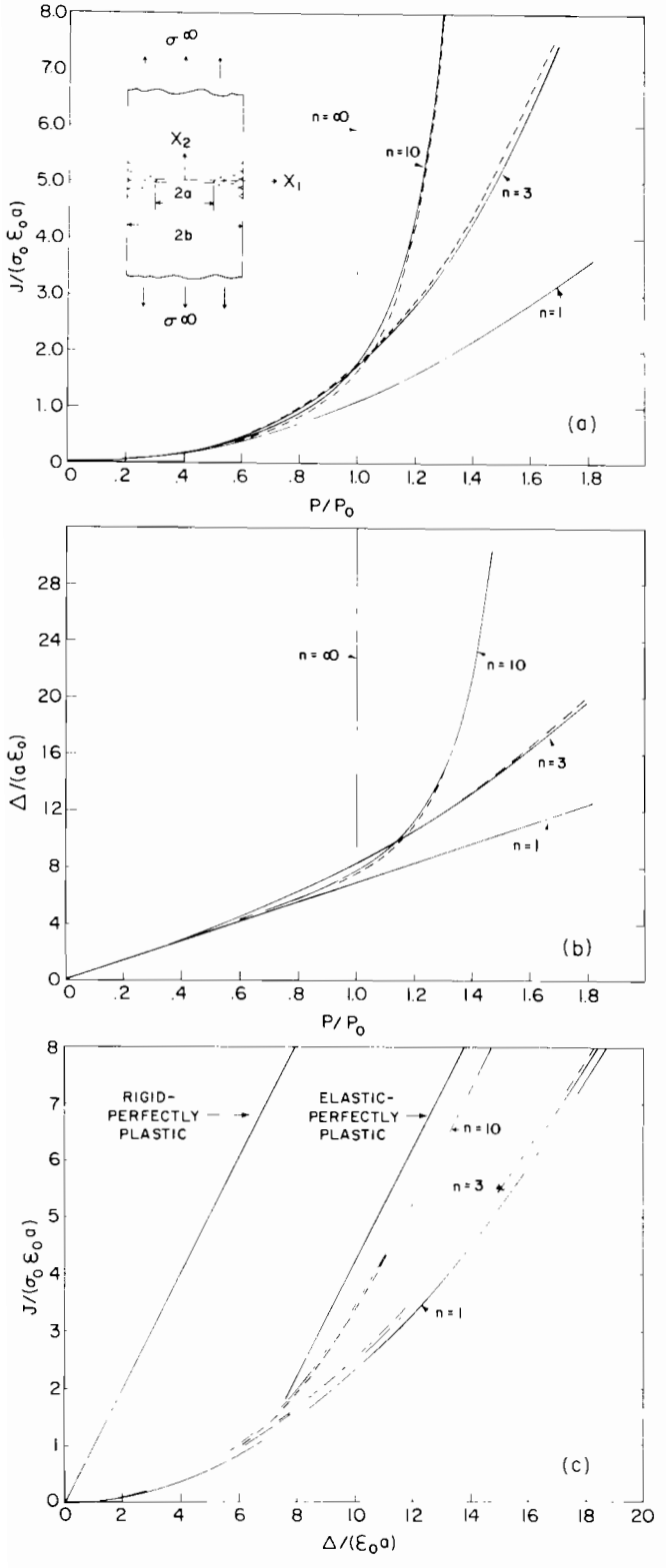


**Fig. 3 Comparison of simple estimates based on formulas (21)-(23) (shown as solid lines) and full numerical calculations (shown as dashed lines) for center cracked strip with $a/b = 1/2$**

Finally, we note that the fully plastic solutions apply to a stationary crack in a material undergoing steady power law creep as discussed in [2].

**Simple Estimates for Elastic/Plastic Behavior and Comparisons With Numerical Calculations.** The formulas for estimating $J$, $\delta$, and $\Delta_c$ for large scale yielding of an elastic/plastic strip are similar to those proposed in [1]. The formulas depend on the choice of tensile stress-strain curve which is used to characterize the material. Use of both Ramberg-Osgood curves and piecewise power hardening curves was discussed in [1]. Here only the former will be considered where

$$\epsilon/\epsilon_0 = \sigma/\sigma_0 + \alpha(\sigma/\sigma_0)^n \quad \text{with} \quad \sigma_0 = E\epsilon_0 \tag{20}$$

With $P$ and $P_0$ still defined as in (6), small scale yielding will prevail as long as $P$ is sufficiently small compared to $P_0$, i.e., the linear elastic formulas will be valid. At the other extreme, when $P$ is large compared to $P_0$, the fully plastic solution can be expected to be a good approximation. To interpolate over the entire range of yielding, we take a sum of the linear and the fully plastic contributions. In addition, to improve the accuracy, the linear contribution is modified using Irwin's idea of a plastically adjusted crack length. Some such modification is clearly needed since, for example, for very large $n$ the fully plastic contribution is negligible for $P < P_0$, yet the linear results start to break down when $P$ exceeds about $P_0/2$, as is well known.

In an abbreviated notation the interpolation formulas are of the form

$$J = J(a_{eff}, n = 1) + J(a, n)$$

where the effective crack length $a_{eff}$ is defined below. Using the quantities defined in (3)–(5), the estimates have the specific forms

$$\frac{J}{\sigma_0\epsilon_0 a(1 - a/b)} = \psi g_1\left[\frac{a_{eff}}{b}, 1\right]\left[\frac{P}{P_0}\right]^2 + \alpha g_1\left[\frac{a}{b}, n\right]\left[\frac{P}{P_0}\right]^{n+1} \tag{21}$$

$$\frac{\delta}{\epsilon_0 a} = \psi g_2\left[\frac{a_{eff}}{b}, 1\right]\frac{P}{P_0} + \alpha g_2\left[\frac{a}{b}, n\right]\left[\frac{P}{P_0}\right]^n \tag{22}$$

$$\frac{\Delta_c}{\epsilon_0 a} = \psi g_3\left[\frac{a_{eff}}{b}, 1\right]\frac{P}{P_0} + \alpha g_3\left[\frac{a}{b}, n\right]\left[\frac{P_0}{P_0}\right]^n \tag{23}$$

where

$$\left.\begin{aligned} a_{eff} &= a + r_y \quad , \; P \le P_0 \\ &= (a_{eff})_{P=P_0} \; , \; P > P_0 \\ r_y &= \frac{1}{2\pi}\left[\frac{n-1}{n+1}\right]\left[\frac{K_I}{\sigma_0}\right]^2 \; , \; \psi = \frac{a_{eff}}{a}\left[\frac{b-a}{b-a_{eff}}\right] \end{aligned}\right\} \tag{24}$$

In (24), Irwin's empirical crack length adjustment $r_y$ for plane stress [6] is taken as an *explicit* function of the elastic stress intensity factor $K_I$. Except for the factor $(n - 1)/(n + 1)$, which accounts for strain hardening [1], the above correction is the same as used in the procedures of [8] and [9] for elastic/perfectly plastic materials. In terms of the present notation $r_y$ can be expressed as

$$r_y/a = (1/2\pi)[(n - 1)/(n + 1)](1 - a/b)g_1(a/b, 1)(P/P_0)^2$$

The factor $\psi$ in the above formulas arises because of the extra terms involving $a$ in the definitions in (3)–(5), including its presence in the definition of $P_0$ in (6). Thus, in (21)–(24) all adjustments have been accounted for and $P_0$ is still defined in terms of the actual crack length $a$ in (6).

Values of $J/(\sigma_0\epsilon_0 a)$ and $\Delta/(\epsilon_0 a)$ as functions of $P/P_0$ calculated from (21), (23), and (9) are shown as solid line curves

in Fig. 3(*a*, *b*) for $a/b = 1/2$, $h/b = 3$, $\alpha = 3/7$ (the choice of Ramberg and Osgood) and for $n = 3$, 10 and $\infty$. The solid line curves in Fig. 3(*c*) for $n = 3$ and 10 are obtained by simply replotting the curves of Figs. 3(*a*) and (*b*) as $J/(\sigma_0\epsilon_0 a)$ against $\Delta/(\epsilon_0 a)$. The curve for $n = \infty$ in Fig. 3(*c*) is the limit result of our procedure as $n \to \infty$. It also coincides with, and is calculated most easily using the procedure suggested for elastic/perfectly plastic materials in [9] and, with a slight modification, in [8]. In each part of Fig. 3 the curves labeled $n = 1$ are the unmodified linear elastic results or, in other words, the small scale yielding predictions.

The dashed line curves in Fig. 3 for $n = 3$ and 10 are the results of a full finite element analysis of the identical strip with $\sigma_{22} = \sigma^\infty$ prescribed on $x_2 = \pm 3b$. This calculation made use of $J_2$ deformation theory fitted to (20) in simple tension with $\alpha = 3/7$. In the plane stress version of this problem $J$ and $\Delta$ can be shown to be independent of Poisson's ratio and $\nu = 1/2$ is a convenient choice for making the calculation. Further details of this calculation are similar to those described for the analogous anti-plane shear problem discussed in the Appendix of [1].

As in the antiplane shear study, the simple formulas compare favorably with the full numerical results. Judging from the success of the approximate formulas, at least in these examples, the Irwin adjustment, although crude, is adequate for the present purpose. In part this is because the influence of the adjustment is relatively small in these examples, as will be discussed further below. The trends revealed in Fig. 3 are similar to those found in anti-plane shear [1]. The most important is the significant effect of even relatively low strain hardening. For example, a hardening exponent of $n = 10$ results in a value of $J$, at a given $\Delta$, which is about 20 percent below the prediction for the elastic/perfectly plastic strip ($n = \infty$) over a significant part of the large scale yielding range. Comparisons were also made for $a/b = 1/4$ with similarly good agreement between the estimates and the full finite element results.

Because of its fundamental importance, we separately list the formula for the limiting case $a/b \to 0$ corresponding to a crack of length $2a$ in an infinite sheet. In this case $P/P_0 = \sigma^\infty/\sigma_0$, $g_1(a/b, 1) = \pi$, $K_I = \sigma^\infty\sqrt{(\pi a)}$ and $\psi = a_{eff}/a$. Equation (21) specializes to

$$\left.\begin{aligned}\frac{J}{\sigma_0\epsilon_0 a} &= \pi\left[1 + \frac{1}{2}\left(\frac{n-1}{n+1}\right)\left(\frac{\sigma^\infty}{\sigma_0}\right)^2\right]\left(\frac{\sigma^\infty}{\sigma_0}\right)^2 + \alpha g_1(0, n)\left(\frac{\sigma^\infty}{\sigma_0}\right)^{n+1} \qquad \sigma^\infty \le \sigma_0 \\ &= \pi\left[1 + \frac{1}{2}\left(\frac{n-1}{n+1}\right)\right]\left(\frac{\sigma^\infty}{\sigma_0}\right)^2 + \alpha g_1(0, n)\left(\frac{\sigma^\infty}{\sigma_0}\right)^{n+1} \qquad \sigma^\infty > \sigma_0\end{aligned}\right\} \tag{25}$$

where $g_1(0, n)$ may be calculated from (16) using the values of $G$ in the table or, from (17), $g_1(0, n) \cong [3.85\sqrt{n}(1 - 1/n) + \pi/n]$. A similar formula can be written for $\delta$. At $\sigma^\infty = \sigma_0$ the contribution due to the Irwin adjustment in (25) amounts to only about 15 percent of the total value when $\alpha = 3/7$ and $n = 5$. At higher values of $\sigma^\infty$ its relative contribution is even less.

## Single Edge-Cracked Strip in Bending

**Fully Plastic Solution.** As depicted in Fig. 4, consider a strip of width $b$ with an edge-crack of length $a$ with an uncracked ligament $c = b - a$. A moment per unit thickness $M$ is applied to the strip; the load-point displacement is denoted by $\theta$ and is approximately the relative rotation of the ends of the strip. Precisely, for a strip of length $2h$ which is free of shearing tractions on its ends and any net load in the 2-direction,

$$M = -\int_0^b x_1\sigma_{22}(x_1, h)dx_1, \quad M\theta(h) = 2\int_0^b \sigma_{22}(x_1, h)u_2(x_1, h)dx_1 \tag{26}$$

The residual load point displacement is defined by

$$\theta_c = \lim_{h\to\infty}[\theta(h) - \theta(h)_{\text{no crack}}] \tag{27}$$

so that for sufficiently large $h$

$$\theta(h) \cong \theta(h)_{\text{no crack}} + \theta_c \tag{28}$$

For the plane stress strip governed by the pure power hardening law (1)

$$\theta(h)_{\text{no crack}} = \frac{4\alpha h\epsilon_0}{b}\left[\left(\frac{2n+1}{n}\right)\frac{2M}{\sigma_0 b^2}\right]^n \tag{29}$$

The limit moment for an edge-cracked, rigid/perfectly plastic strip ($n \to \infty$) is given by [10]

$$M_0 = 0.2679\, c^2\sigma_0 \tag{30}$$

as long as $a/b$ is not too small. The associated slip line field is indicated in the insert of Fig. 4. The moment quantity $M_0$ defined by (30) is used as the reference value in the following normalizations for the infinite edge-cracked strip in bending:

$$J = \alpha\sigma_0\epsilon_0 c h_1(a/b, n)(M/M_0)^{n+1} \tag{31}$$

$$\delta = \alpha\epsilon_0 a h_2(a/b, n)(M/M_0)^n \tag{32}$$

$$\theta_c = \alpha\epsilon_0 h_3(a/b, n)(M/M_0)^n \tag{33}$$

where $\delta = u_2(0, 0^+) - u_2(0, 0^-)$ is the crack opening displacement at the edge of the strip.

Values of $h_1$, $h_2$, and $h_3$ are given in Table 2 for the single geometry ratio $a/b = 1/2$. If desired, $h_1$, $h_2$, and $h_3$ can be expressed in terms of approximate analytic formulas in [6] for $n = 1$. We will argue below that, for $n$ greater than about 3, the values for $a/b = 1/2$ are accurate to within a few percent for all more deeply notched specimens, i.e., for $a/b > 1/2$. For

**Table 2**

| $a/b = 1/2$ | $1/n = 1$<br>$n = 1$ | 0.5<br>2 | 0.333<br>3 | 0.2<br>5 | 0.143<br>7 | 0.1<br>10 |
|---|---|---|---|---|---|---|
| $h_1$ | 1.104 | 0.957 | 0.851 | 0.717 | 0.653 | 0.551 |
| $h_2$ | 5.129 | 3.640 | 2.947 | 2.255 | 1.953 | 1.606 |
| $h_3$ | 2.749 | 2.359 | 2.032 | 1.590 | 1.373 | 1.121 |

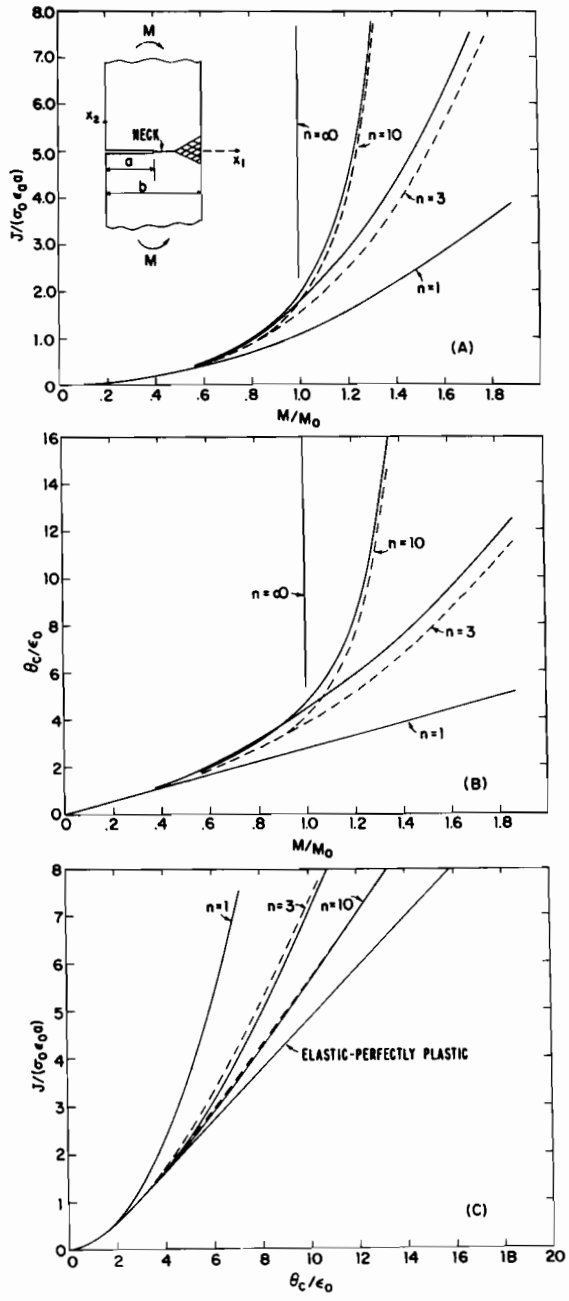


**Fig. 4 Comparison of simple estimates based on formulas (38)-(40) (shown as solid lines) and full numerical calculations (shown as dashed lines) for single edge cracked strip in bending with $a/b = 1/2$**

the linear case, $h_1(1/2, 1) = 1.104$ is already within 3 percent of the deeply notched value $h_1(1, 1) = 1.135$ from [6]. On the other hand, $h_2(a/b, 1)$ and $h_3(a/b, 1)$ are equally good approximations to the corresponding deeply notched values only for $a/b$ greater than about 3/4. Since the effect of $n > 1$ is to localize the deformation to the region ahead of the crack, one would expect the case $a/b = 1/2$ should serve as a good approximation to the deeply notched bend specimen if $n$ is sufficiently large. An independent connection between $J$, $M$, and $\theta_c$ for deeply notched specimens provides a means of assessing how large $n$ must be.

It has been shown in [9] that the integral,

$$I = (2/c)_0 \int_0^{\theta_c} M d\theta_c \tag{34}$$

has the property that $I \to J$ as $a/b \to 1$. That is, (34) is an alternative expression for $J$ for deeply notched specimens. Now, we evaluate $I$ using the present fully plastic results for $a/b = 1/2$ and see how closely $I$ agrees with $J$ for various $n$. With (33) in (34),

$$I = 0.5358(n/n + 1)\alpha\sigma_0\epsilon_0 c h_3 (M/M_0)^{n+1} \tag{35}$$

The ratio $I/J$ is, from (35) and (31),

$$I/J = 0.5358\, n h_3/[(n + 1)h_1] \tag{36}$$

The plot of $I/J$ against $1/n$ in Fig. 5 is obtained from the numeri-

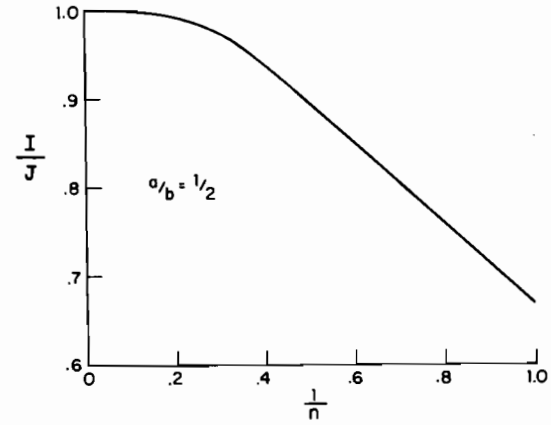


**Fig. 5 Values of I/J from equation (36)**

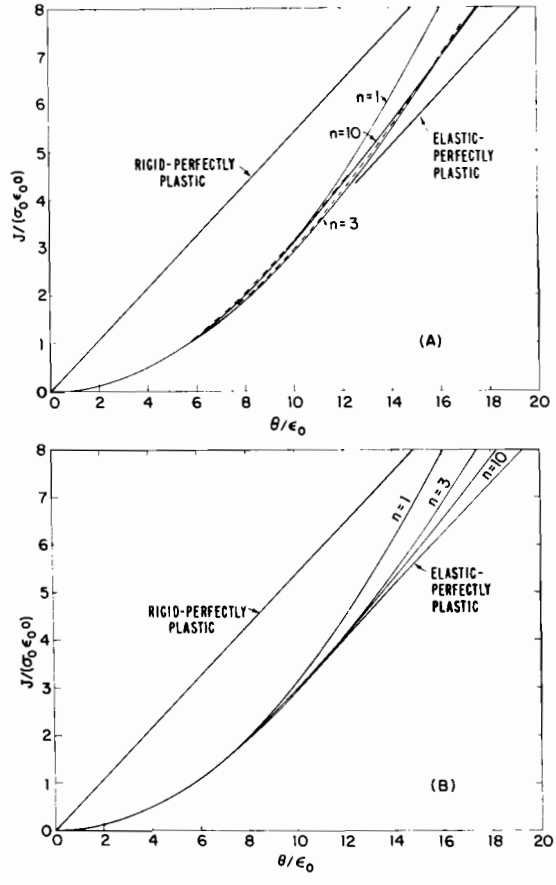


**Fig. 6 Effect of strain hardening and shape of stress strain curve on relation between $J$ and $\theta$ for a plane stress bend specimen. (a) Based on Ramberg-Osgood stress strain curve (20). (b) Based on piecewise power hardening curve (41). (Solid line curves based on estimation formulas, dashed line curves based on full numerical calculations.)**

cal values of $h_1(1/2, n)$ and $h_3(1/2, n)$ in Table 2. For $n \geq 3$ $I$ is within 3 percent of $J$. We interpret this as indicating that the strip can be regarded as deeply notched under fully plastic conditions with $n \geq 3$ if $a/b \geq 1/2$. Finally, note the rigid/perfectly plastic limit result ($n \to \infty$) from (34)

$$J = (2/c)M_0\theta_c \tag{37}$$

which is otherwise independent of $a/b$, assuming $a/b$ is not very small.

**Estimates for Elastic/Plastic Specimens and Comparisons With Numerical Calculations.** The formulas for estimating $J$, $\delta$, and $\theta_c$, for a strip of material that has tensile properties (20), are arrived at in the same way as discussed for the center-cracked strip. They are

$$\frac{J}{\sigma_0\epsilon_0 c} = \psi^2 h_1\left(\frac{a_{eff}}{b}, 1\right)\left(\frac{M}{M_0}\right)^2 + \alpha h_1\left(\frac{a}{b}, n\right)\left(\frac{M}{M_0}\right)^{n+1} \tag{38}$$

$$\frac{\delta}{\epsilon_0 a} = \psi^2 \frac{a_{eff}}{a} h_2\left(\frac{a_{eff}}{b}, 1\right)\frac{M}{M_0} + \alpha h_2\left(\frac{a}{b}, n\right)\left(\frac{M}{M_0}\right)^n \tag{39}$$

$$\frac{\theta_c}{\alpha\epsilon_0} = \psi^2 h_3\left(\frac{a_{eff}}{b}, 1\right)\frac{M}{M_0} + \alpha h_3\left(\frac{a}{b}, n\right)\left(\frac{M}{M_0}\right)^n \tag{40}$$

where, now, $\psi = (b - a)/(b - a_{eff})$ and $a_{eff}$ is defined by (24) with $P$ and $P_0$ replaced by $M$ and $M_0$, respectively. In the above formulas $M_0$ is defined in terms of the actual uncracked ligament length $c$ in (30).

Plots of $J$ and $\theta_c$ as functions of $M/M_0$ as calculated from (38) and (40) are shown as solid line curves in Figs. 4($a$), ($b$) for $a/b = 1/2$, $\alpha = 3/7$ and $n = 3$ and 10. Curves of $J$ against $\theta_c$ are shown in Fig. 4($c$). The curves for $n = 1$ are the unadjusted elastic results (i.e., the small scale yielding predictions) and those for $n = \infty$ are the limit of the present estimation procedure which coincides with that of [9]. Dashed line curves in Fig. 4 are the result of a full finite element analysis of a specimen whose material, as in the center-cracked case, is governed by (20) in simple tension and is generalized using $J_2$ deformation theory. In these calculations $h/b = 2$ was taken and $\theta_c$ was calculated according to its definition in (27) using the approximation (28) for a finite length strip.

For the bend specimen the comparison of the simple estimates with the full numerical calculations is not quite as favorable as in the case of the center-cracked specimen. Apparently this is because of the relatively larger contribution of the Irwin correction in this problem. Significantly, however, the discrepancy for the relation of $J$ to $\theta_c$ is almost negligible and evidently not strongly affected by the approximate character of the Irwin adjustment.

For testing, the relation of $J$ to $\theta$ is of particular interest [11]. Given $\theta_c$ as a function of $M/M_0$ in (40), $\theta$ can be calculated using (28), where now $\theta(h)_{\text{no crack}}$ must be calculated for the pure bending of the uncracked strip of length $2h$ composed of material satisfying (20). The result in the form of $J$ as a function of $\theta$ is shown in Fig. 6($a$) for $h/b = 2$. As before the solid lines are based on the estimates and the dashed lines are the results of the full numerical calculation. Over the range shown the effect of strain hardening is not unduly large in this relationship. To obtain the curves of Fig. 6($b$), we have used the estimation procedure for the piecewise-power hardening tensile curve given in [1]. The tensile behavior in this case is

$$\begin{aligned} \epsilon/\epsilon_0 &= \sigma/\sigma_0 \quad , \ \sigma \leq \sigma_0 \\ &= (\sigma/\sigma_0)^n \ , \ \sigma > \sigma_0 \end{aligned} \qquad (\sigma_0 = E\epsilon_0) \tag{41}$$

The curves in Fig. 6 illustrate the extent to which the shape of the stress-strain curve can influence the relation between $J$ and $\theta$ independent of the strain hardening exponent $n$. It is also interesting to note that, at a given $\theta$, $J$ decreases with increasing $n$ as opposed to the trend for given $\Delta$ in Fig. 3($c$).

## References


1 Shih, C. F., "J Integral Estimates for Strain Hardening Materials in Antiplane Shear using Fully Plastic Solutions," in *Mechanics of Crack Growth*, ASTM STP 590, 1976, 3-22.

2 Goldman, N. L., and Hutchinson, J. W., "Fully Plastic Crack Problems: The Center-Cracked Strip under Plane Strain," *Int. J. Solids Structures*, 1975, Vol. 11, pp. 575–591.

3 Rice, J. R., "Mathematical Analysis in the Mechanics of Fracture," in *Fracture* (ed. by H. Liebowitz), 1968, Vol. II, Academic Press, New York, pp. 191–311.

4 Amazigo, J. C., "Fully Plastic Crack in an Infinite Body under Anti-plane Shear," *Int. J. Solids Structures*, 1974, Vol. 10, p. 1003.

5 Benthem, J. P., and Koiter, W. T., "Asymptotic Approximations to Crack Problems," in *Mechanics of Fracture*, (ed. by G. C. Sih), 1973, Noordhoff Leyden.

6 Tada, H., Paris, P., and Irwin, G., *The Stress Analysis of Cracks Handbook*, published by the Del Research Corporation, 1973.

7 Amazigo, J. C., "Fully Plastic Center-Cracked Strip Under Anti-Plane Shear," *Int. J. Solids Structures*, Vol. 11, 1975, pp. 1291-1299.

8 Bucci, R. J., Paris, P. C., Landes, J. D. and Rice, J. R., "J Integral Estimation Procedures," in *Fracture Toughness*, ASTM STP 514, 1972, pp. 40–69.

9 Rice, J. R., Paris, P. C., and Merkle, J. G., "Some Further Results of J-Integral Analysis and Estimates," in *Progress in Flaw Growth and Fracture Toughness Testing*, ASTM STP 536, 1973, pp. 231–245.

10 Ford, H., and Lianis, G., *Z. Agnew. Math. Phys.*, 1957, Vol. 8, pp. 360–382.

11 Begley, J. A., and Landes, J. D., "The J Integral as a Fracture Criterion," in *Fracture Toughness*, ASTM STP 514, 1972, pp. 1–20.